Simultaneous Hallucination and Recognition of Low-Resolution Faces Based on Singular Value Decomposition

Muwei Jian and Kin-Man Lam, *Senior Member, IEEE*

***Abstract*— In video surveillance, the captured face images are usually of low resolution (LR). Thus, a framework based on singular value decomposition (SVD) for performing both face hallucination and recognition simultaneously is proposed in this paper. Conventionally, LR face recognition is carried out by super-resolving the LR input face first, and then performing face recognition to identify the input face. By considering face hallucination and recognition simultaneously, the accuracy of both the hallucination and the recognition can be improved. In this paper, singular values are first proved to be effective for representing face images, and the singular values of a face image at different resolutions have approximately a linear relation. In our algorithm, each face image is represented using SVD. For each LR input face, the corresponding LR and high-resolution (HR) face-image pairs can then be selected from the face gallery. Based on these selected LR–HR pairs, the mapping functions for interpolating the two matrices in the SVD representation for the reconstruction of HR face images can be learned more accurately. Therefore, the final estimation of the high-frequency details of the HR face images will become more reliable and effective. The experimental results demonstrate that our proposed framework can achieve promising results for both face hallucination and recognition.**

***Index Terms*— Face hallucination, low-resolution (LR) face recognition, mapping model, singular value decomposition (SVD).**

I. Introduction

FACE recognition is an important task in video surveillance. The two primary tasks of face recognition are face identification and verification. In face identification, a query face is compared with the gallery faces in a data set so as to determine its identity. For face verification, the claimed identity of a query face is verified. Face recognition can achieve a highly accurate performance under controlled conditions, such as under frontal light sources, frontal view, no occlusion, and neutral facial expression. However, low-resolution (LR) faces are a difficult problem in the face-recognition domain. Although current digital cameras can capture images at high resolution (HR), face images captured in outdoor circumstances and at a distance, with a compressed video format, are usually of LR and low quality. To achieve effective video surveillance, both face hallucination and face recognition are needed simultaneously.

In the image-processing research field, reconstruction of a HR image from its LR inputs is called superresolution (SR). For face images, this technology is also called face hallucination [1], which has become one of the most important fields of face recognition. Face hallucination was first proposed in [1], and has drawn many researchers' attention since then. A pixel-wise SR method was proposed in [1], which uses the Laplacian and the Gaussian pyramids to decompose an image into a pyramid of features to generate an HR face image. Later, the limitations of SR, and how to break the limitations, were introduced in [2]. Freeman *et al.* [3] proposed a nonparametric patch-based prior combined with the Markov random field model to produce the desired HR images. In [4], temporal correspondence and a prior model were combined to hallucinate faces. References [5]–[7] and [11] have further developed patch-based SR frameworks. A sparse-coding method [7] was proposed to represent an LR input patch as a combination of its raw, neighboring image patches; the target HR patch is generated directly using the same combination coefficients for the corresponding neighboring HR patches. The algorithms proposed in [5] and [6] also used the same approach, in which a number of similar neighbors to the LR input patches are searched from a training data set, and then a specific method is adopted to reconstruct the corresponding HR images. Wang and Tang [8] proposed a holistic face-hallucination method that employs principal component analysis (PCA) to represent an LR input image as a linear combination of LR training samples. The corresponding HR image is then estimated using the same linear combination of the corresponding HR training samples. Park and Lee [9] utilized the PCA-based SR framework [8] to develop an example-based face-hallucination method. As the PCA method considers global-structural information about facial images, it is less suitable for use in patch-based approaches [12]. In [10], a hybrid method was proposed, based on global and local constraints, for applying face hallucination to unregistered images. In [11], a novel example-based image SR method was proposed, in which a class-specific predictor is designed for each class of patches so as to improve the accuracy of estimating the missing high-frequency content. Another early learning-based SR technique was developed in [12] and [13]. These methods

Manuscript received May 31, 2014; revised August 28, 2014 and December 9, 2014; accepted February 3, 2015. Date of publication February 9, 2015; date of current version October 28, 2015. This paper was recommended by Associate Editor S. Yan.

M. Jian is with the Department of Computer Science and Technology, Ocean University of China, Qingdao 266100, China, and also with the Centre for Signal Processing, Department of Electronic and Information Engineering, The Hong Kong Polytechnic University, Hong Kong (e-mail: jianmuwei@ouc.edu.cn; 10902666r@connect.polyu.hk).

K.-M. Lam is with the Centre for Signal Processing, Department of Electronic and Information Engineering, The Hong Kong Polytechnic University, Hong Kong (e-mail: enkmlam@polyu.edu.hk).

Color versions of one or more of the figures in this paper are available online at http://ieeexplore.ieee.org.

Digital Object Identifier 10.1109/TCSVT.2015.2400772

are based on the observation that, for an LR version of an image that visually resembles its HR counterpart, the LR and its corresponding HR image should be intrinsically correlated. In other words, the LR image can be used as an input to predict its HR counterpart. Ma *et al.* [14] proposed a method to hallucinate HR image patches using patches at the same position in each training image. Then, the optimal weights for the training position patches are estimated, and are used to reconstruct the corresponding HR patches. Recently, a new face-hallucination framework—namely, from local-pixel structure to global image SR—was developed in [15], and is based on the assumption that two similar face images should have similar local-pixel structures. This new framework uses an input LR face image to search a face database for similar example HR faces to learn the local-pixel structures for the target HR face. In [16], a synthesized approach that utilizes both the shape and the texture components was proposed. These two components are based on accurately aligned local image regions. To achieve sufficient accuracy in alignment, shape reconstruction is solved together with texture reconstruction in a coordinated manner.

To investigate the problem of unconstrained face recognition, the Labeled Faces in the Wild (LFW) database was designed to evaluate the performance of different algorithms. The LFW database consists of real-world face images, which were collected in the wild with different poses, lighting conditions, resolutions, qualities, expressions, gender, races, occlusions, and make-up [41]. Later, different types of aligned images became available, namely, the LFW funneled images (the LFW images aligned by funneling [42]) and the LFW deep-funneled images (the LFW images aligned by deep funneling [43]), to evaluate the performance of different face recognition algorithms.

Currently, most existing methods focus only on face reconstruction, and seldom consider face recognition and hallucination simultaneously. In [17], an approach for simultaneous face SR and feature extraction for LR face verification was proposed. This approach simultaneously provides fitness measures of the SR results from both the reconstruction and recognition perspectives. Zou and Yuen [37] proposed an approach to learning the relationship between the HR image space and the very LR image space for face SR. The proposed discriminative SR (DSR) method, with a discriminative constraint, is used to learn the proper relationship, based on class information, for face-recognition applications.

In contrast to the previous work on face-hallucination [36], we investigate the two important issues, i.e., face hallucination and face recognition, simultaneously. Most existing methods focus on constructing HR faces followed by face recognition, i.e., in two separate and independent steps, for LR face recognition. In this paper, the core contribution is that we have extended a face-hallucination technique so that both face recognition and hallucination are considered simultaneously. In particular, a novel and efficient scheme is proposed for the simultaneous hallucination and recognition of LR face images via singular value decomposition (SVD) and a LR–HR mapping model for the SVD representation. In our approach, face images are represented using SVD, and the hallucination and recognition of LR faces are considered simultaneously. We have proved [36] that, based on the Frobenius norm, the corresponding singular values of an image across different resolutions have approximately a linear relationship. This makes the estimation of the singular values of HR face images more reliable. Furthermore, the left and right matrices in the SVD representation can be interpolated to a higher resolution using bicubic interpolation [29]; this interpolation method applied to these two matrices will not change the holistic structure or the pattern of the face image. Our proposed approach can be applied to both face verification and identification.

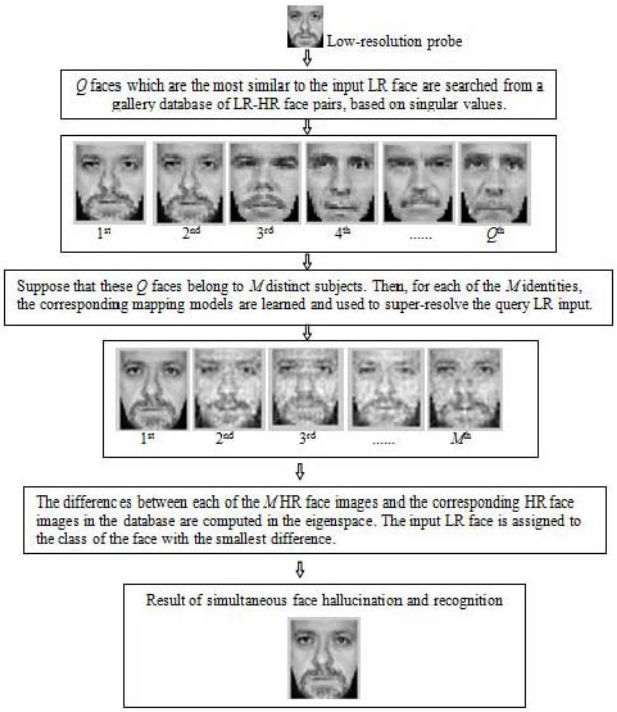

Fig. 1. Proposed framework for the simultaneous hallucination and identification of LR faces based on SVD and a mapping-model method.

Our simultaneous face-hallucination and face-verification algorithm is denoted by SHV. As the claimed identity of the query is known, the claim will simply be rejected if the difference between the singular values of the query and those of the claimed faces in the database is larger than a certain threshold. If the difference is smaller than the threshold, SR will be performed based on the mapping models learned from the claimed LR–HR face pairs. The LR-to-HR mapping matrices of the respective claimed face pairs are learned for estimating the high-frequency information or any detailed local features missed in the estimated HR faces generated by interpolating the two SVD matrices. The hallucinated faces are then used for verification again. On the other hand, the algorithm for simultaneous face hallucination and identification is denoted by SHI. In this algorithm, the Q faces that are the most similar to the input LR face image are first searched from a gallery database of LR–HR pairs, based on its singular values. Suppose that these Q faces belong to M distinct subjects, where $M < Q$. For each of these M identities, the

corresponding mapping models are learned and used to super-resolve the query input. Therefore, M HR face images for the LR query are generated. Then, the differences between each of the M HR face images and the corresponding HR face images in the database are computed based on PCA. The input LR face is assigned to the class of the face with the smallest difference. Fig. 1 shows the proposed framework for the simultaneous hallucination and identification of LR faces based on SVD and the LR-to-HR mapping models.

As is well known, for a novel face that is significantly different from the training samples, most of the existing learning-based face-hallucination methods will likely produce artifacts and discontinuities in the reconstruction results. The face-recognition steps in the proposed approach have the advantage that the above-mentioned problem can be solved to a certain extent. If the referred faces do not have similar holistic structures and patterns to the LR input, these faces will be rejected during face recognition. Concurrently, with the aid of face recognition, the estimation of the high-frequency details of the HR face images will become more reliable and effective.

The rest of this paper is organized as follows. In Section II, we will present a simple mapping model for hallucinating SVD matrices. Section III introduces our proposed face-hallucination and -recognition scheme. The experimental results are presented in Section IV, and this paper closes with the conclusion and discussion in Section V.

II. Singular Value Decomposition and the Mapping Model

A. Singular Value Decomposition of Face Images

In this section, we use a mathematical framework to achieve an effective image representation for face hallucination [36]. Our proposed framework projects an image I of size $m \times n$ on to the eigenspace using SVD. The image I can be viewed as a matrix with m rows and n columns. Using SVD, I can be decomposed as

$$I = UWV^T \tag{1}$$

where $U^TU = V^TV = E$, and E is an identity matrix. The matrix U is a $m \times m$ column-orthogonal matrix, while V is a $n \times n$ orthogonal matrix. The elements w_i on the diagonal of W are called singular values (the square root of the eigenvalues)

$$W = \mathrm{diag}(w_1, w_2, \ldots, w_i, \ldots, w_n). \tag{2}$$

The singular value vector s of the image I is defined as

$$s = [w_1, w_2, \ldots, w_i, \ldots, w_n]^T \tag{3}$$

where $1 \le i \le n$, and w_i is the ith singular value of I in the singular value vector s such that $w_i \ge w_{i+1}$. It can be observed that the singular values decrease dramatically. The following definitions can be used to measure the information accounted for by the ith eigenvector [18]:

$$f_{\mathrm{indi}}(i) = \sqrt{\frac{w_i^2}{\sum_{i=1}^{n} w_i^2}} \tag{4}$$

and the accumulation of the first k eigenvectors [19] can be measured as

$$f_{\mathrm{cumu}}(k) = \sqrt{\frac{\sum_{i=1}^{k} w_i^2}{\sum_{i=1}^{n} w_i^2}}. \tag{5}$$

In general, the first several eigenvectors are sufficient to account for almost all of the information contained in an image. This observation is also true for texture images [20], [21] and face images [36], [39].

Since the singular values decrease rapidly and the first few eigenvectors can account for most of the information, the original matrix W can be approximated as $\hat{W}_I$ as

$$\hat{W}_I = \mathrm{diag}(w_1, w_2, \ldots, w_k, 0, \ldots, 0) \tag{6}$$

and we have

$$\sum_{i=1}^{n} w_i^2 \cong \sum_{i=1}^{k} w_i^2 \tag{7}$$

where k is the number of singular values or eigenvectors to be retained. We choose the first k singular values, rather than all the n nonzero singular values available, because those high-order singular values represent the high-frequency content, or noise, in the interpolated LR face image under consideration. Based on the first k singular values, we can obtain an approximated image $\hat{I}$ that contains almost the same information as the original image I. The image $\hat{I}$, which can be viewed as a matrix, can be expressed as

$$\hat{I} = U\hat{W}_I V^T. \tag{8}$$

B. Diagonal Matrix W at Different Resolutions

According to [22] and [36], if a matrix A has singular values w_1, where $1 \le i \le n$, then

$$||A||_F = \sqrt{\sum_{i=1}^{n} w_i^2} \tag{9}$$

where $\|A\|_F$ is the Frobenius norm of the matrix A, which is defined as the square root of the sum of the squares of all its entries. The proof of (9) can be found in [36].

Furthermore, we observe that when an LR image I_l is interpolated or super-resolved to produce a new HR image I_h with a magnification factor of α, the first k leading singular values in the singular-value vector $s_h = [w_h^1, w_h^2, \ldots, w_h^k]^T$, of the image I_h can be approximated as α times of the first k leading singular values in the singular value vector $s_l = [w_l^1, w_l^2, \ldots, w_l^k]^T$, of the original image I_l. Hence, we have

$$s_h \cong \alpha s_l. \tag{10}$$

In other words, the leading singular values of the sam e image under different resolutions are approximately proportional to each other, with the magnification factor α as the proportional constant.

Theorem 1: If an LR image I_l is interpolated to produce an HR image I_h with a magnification factor of α, then the first k leading singular values in the singular-value vector

s_h of the new image I_h are α times the corresponding first k leading singular values of the singular-value vector s_l of the original image I_l.

Proof: Suppose that I_l is interpolated to produce a new HR image I_h with a magnification factor of α, then we have

$$\begin{aligned}\|\mathrm{I}_h\|_F^2 &\overset{[1]}{\cong} \|\alpha I_l\|_F^2 = a^2\|I_l\|_F^2 \\ &\overset{[2]}{=} \alpha^2 \sum_{i=1}^{n} \left(w_l^i\right)^2 \\ &\overset{[3]}{\cong} \alpha^2 \sum_{i=1}^{k} \left(w_l^i\right)^2 = \sum_{i=1}^{k} \left(\alpha w_l^i\right)^2 = \sum_{i=1}^{k} \left(w_h^i\right)^2 \\ s_h &\overset{[4]}{\cong} \alpha s_l.\end{aligned}$$

1) An interpolation method, with a magnification factor of α, produces $\alpha \times \alpha$ neighboring pixels in the interpolated image I_h with similar values to the corresponding pixel in the original LR image I_l. For instance, the nearest-neighbor interpolation generates $\alpha \times \alpha$ neighbors of equal values, and the bilinear and bicubic-interpolation methods produce $\alpha \times \alpha$ similar pixels.

2) According to (9), $\|A\|_F^2 = \sum_{i=1}^{n} w_i^2$.

3) According to (7), $\sum_{i=1}^{n} w_i^2 = \sum_{i=1}^{k} w_i^2$.

4) By linear algebra, the spectral norm (i.e., the Euclidean norm) of the matrix A is the largest singular value of A

$$||A||_2 = w_1.$$

For image I_h and the original LR image I_l, we have

$$\begin{aligned}||I_h||_2 &= w_h^1 \quad \text{and} \\ ||I_l||_2 &= w_l^1.\end{aligned}$$

Since the image I_h, with a magnification factor of α, has similar values to the corresponding pixel in the original LR image I_l, we have $\|I_h\|_2 \cong \|\alpha I_l\|_2 = a\|I_l\|_2$. This is equivalent to

$$w_h^1 \cong \alpha w_l^1.$$

Then, the linear relationship becomes

$$\sum_{i=2}^{k} \left(w_h^i\right)^2 \cong \alpha^2 \sum_{i=2}^{k} \left(w_l^i\right)^2.$$

Now, we can set $w_h^1 = 0$ and $w_l^1 = 0$, the new image $I_h^{'}$ and $I_l^{'}$ can be expressed as

$$I_h^{'} = U_h \begin{pmatrix} 0 & & & & \\ & w_h^2 & & & \\ & & \cdots & & \\ & & & w_h^k & \\ & & & & 0 \\ & & & & & 0 \end{pmatrix} V_h^T \quad \text{and}$$

$$I_l^{'} = U_l \begin{pmatrix} 0 & & & & \\ & w_l^2 & & & \\ & & \cdots & & \\ & & & w_l^k & \\ & & & & 0 \\ & & & & & 0 \end{pmatrix} V_l^T.$$

The Euclidean norms of the matrix $I_h^{'}$ and $I_l^{'}$ are their corresponding largest singular values as

$$\begin{aligned}||I_h^{'}||_2 &= w_h^2 \quad \text{and} \\ ||I_l^{'}||_2 &= w_l^2.\end{aligned}$$

Similarly, since $||I_h^{'}||_2 \cong ||\alpha I_l^{'}||_2 = \alpha||I_l^{'}||_2$, we have

$$w_h^2 \cong \alpha w_l^2.$$

Therefore, the linear relationship becomes

$$\sum_{i=3}^{k} \left(w_h^i\right)^2 \cong \alpha^2 \sum_{i=3}^{k} \left(w_l^i\right)^2.$$

Using the principle of mathematical induction, we can also set $w_h^1 = 0$, $w_h^2 = 0$ and $w_i^1 = 0$, $w_l^2 = 0$. Thus, we have

$$\begin{aligned}w_h^3 &\cong \alpha w_l^3 \quad \text{until} \\ w_h^k &\cong \alpha w_l^k.\end{aligned}$$

This proves (10), which means that the leading singular values of the same image under different resolutions are approximately proportional to each other with the magnification factor α. In addition, since the Euclidean norm of the matrix A is the largest singular value of A [22], [39], and with (10), we can utilize the largest singular value w_h^1 of I_h and the largest singular value w_l^1 of the original LR image I_l, respectively, to normalize the global feature to form scale-invariant feature vectors as

$$s_h' = \frac{s_h}{w_h^1} \quad \text{and} \quad s_l' = \frac{s_l}{w_l^1}. \tag{11}$$

We can see that $s_h' = s_l'$, which means that the singular values are normalized so that face images at different resolutions can be compared directly [39].

C. Proposed Mapping Model: Mapping U and V in the Eigenspace

Suppose that an HR face image is denoted by I_h and the corresponding LR image is denoted by I_l. These two images, I_h and I_l, can be expressed in the eigenspace using SVD as follows [36]:

$$I_h = U_h W_h V_h^T \quad \text{and} \tag{12}$$

$$I_l = U_l W_l V_l^T. \tag{13}$$

The two matrices U_l and V_l for I_l can be interpolated using the bicubic algorithm [29] to form two new matrices U_l' and V_l' that have the same size as U_h and V_h, respectively. Define two mapping matrices P_u and P_v, as

$$U_h = U_l' P_u \quad \text{and} \tag{14}$$

$$V_h = V_l' P_v. \tag{15}$$

The two matrices P_u and P_v can be computed approximately as

$$\tilde{P}_u = \left(U_l^{'T} U_l^{'} + \varepsilon E\right)^{-1} U_l^{'T} U_h \quad \text{and} \tag{16}$$

$$\tilde{P}_v = \left(V_l^{'T} V_l^{'} + \varepsilon E\right)^{-1} V_l^{'T} V_h \tag{17}$$

where ε is a small positive integer and E is a unit matrix. An estimation of U_h and V_h, denoted by $\hat{U}_h$ and $\hat{V}_h$, respectively, can be expressed as

$$\hat{U}_h = U_l' \tilde{P}_u \quad \text{and} \tag{18}$$

$$\hat{V}_h = V_l' \tilde{P}_v. \tag{19}$$

For the purpose of SR, an HR image can be reconstructed from a LR image using the matrices $\hat{U}_h$ and $\hat{V}_h$, which can be learned from a pair of LR–HR training face images; and the diagonal matrix $\hat{W}_h$ is computed using the scheme described in Section II-B. Thus, we have

$$I_h = \hat{U}_h \hat{W}_h \hat{V}_h^T. \tag{20}$$

III. Simultaneous Hallucination and Recognition of Low-Resolution Faces

For simultaneous face hallucination and face recognition, we consider the algorithms HSV and HSI separately. The major difference between these two algorithms is in the selection of the LR–HR training pairs when performing face SR for face verification and identification.

A. Simultaneous Face Hallucination and Verification (SHV)

Given a pair of face images, the task of face verification is to verify whether they belong to the same person or not. In our framework for SHV, we will first use the singular values of face images as a global scale-invariant feature vector for their representation according to (11). We define a similarity function, SIM, to measure the similarity between an input query and the claimed identity in the gallery database, based on singular values only, as

$$\mathrm{SIM}(I_1, I_2) = \frac{1}{\left\| s_{I_1}' - s_{I_2}' \right\|_2} \tag{21}$$

where $\| \ \|_2$ is the L_2 norm, and s_{I_1}' and s_{I_2}' are the normalized leading singular values utilizing the largest singular value, i.e., (11), of the input LR probe and the claimed identity in the gallery database, respectively. If the difference between the singular values of the query and the claimed identity is larger than a certain threshold, i.e., SIM $\leq T_1$, the claimed face will be rejected. If the difference is smaller than the threshold, i.e., SIM $> T_1$, SR will be performed based on the mapping models learned from the claimed LR–HR face pairs. The threshold T_1 is empirically set by experiments. Then, the face hallucination of the input LR face, using only the claimed face pairs as references to estimate the mapping functions for interpolating the two matrices in the SVD representation, is described in the following.

Suppose that N face images of the claimed identity in the gallery set can pass the face-verification process based on singular values, and that the face images in the gallery are $\alpha \times \alpha$ times the input LR face image I_l. These N face images are downsampled to form N pairs of LR and HR training face images, denoted by I_l^i and I_h^i $(i = 1, \ldots, N)$, respectively. The LR training images should have a high structural similarity to the LR input face after alignment. Based on the N face pairs, N corresponding HR face images can be reconstructed from the LR face using the mapping model scheme described in Section II-B

$$\hat{U}_h^i = U_l'^i \tilde{P}_u^i \quad \text{and} \tag{22}$$

$$\hat{V}_h^i = V_l'^i \tilde{P}_v^i \tag{23}$$

where $1 \leq i \leq N$.

We can now learn the mapping matrices $\tilde{P}_u$ and $\tilde{P}_v$ for face hallucination using the individual mapping matrices $\tilde{P}_u^i$ and $\tilde{P}_v^i$, learned from the N pairs of HR and LR images. A linear combination of the mapping matrices can be written as follows:

$$\tilde{P}_u = \sum_{i=1}^{N} \beta_i \tilde{P}_u^i \quad \text{and} \tag{24}$$

$$\tilde{P}_v = \sum_{i=1}^{N} \gamma_i \tilde{P}_v^i \tag{25}$$

where β_i and γ_i are the embedding coefficients [36] for $\tilde{P}_u$ and $\tilde{P}_v$, respectively.

After the LR input image I_l is decomposed by SVD using (12), its U_l and V_l can be interpolated to generate two new matrices U_l' and V_l' with the same size as U_h and V_h for the desired HR image I_h, respectively. Then, the corresponding approximated matrices $\hat{U}_h$ and $\hat{V}_h$ can be computed as follows:

$$\hat{U}_h = U_l' \tilde{P}_u \quad \text{and} \tag{26}$$

$$\hat{V}_h = V_l' \tilde{P}_v. \tag{27}$$

As described in Section II-B, the leading singular values in the diagonal matrix $\hat{W}_h$ can be estimated using the linear relationship $s_h \cong \alpha s_l$. The number of leading singular values k to be used can be determined using (5), such that the first k leading singular values can represent a sufficient amount of information about the face images. In our algorithm, we choose $f_{\mathrm{cumu}}(k) \geq \eta$ (where $\eta = 0.99$ in our experiment). After estimating the first k leading singular values, we can also estimate the remaining singular values, denoted by $s_h'(k) = [w_h^{k+1}, w_h^{k+2}, \ldots, w_h^{\alpha n}]^T$, in the diagonal matrix $\hat{W}_h$ using a linear combination of the remaining singular values $s_h'^i(k) = [w_h^{i,k+1}, w_h^{i,k+2}, \ldots, w_h^{i,\alpha n}]^T$ of the N similar HR images as

$$\begin{aligned} s_h'(k) &= \left[w_h^{k+1}, w_h^{k+2}, \ldots, w_h^{\alpha n}\right]^T \\ &= \sum_{i=1}^{N} \zeta_i s_h'^i = \sum_{i=1}^{N} \zeta_i \left[w_h^{i,k+1}, w_h^{i,k+2}, \ldots, w_h^{i,\alpha n}\right]^T. \end{aligned} \tag{28}$$

Now, the HR image $\hat{I}_h$ can be reconstructed using the estimated matrices $\hat{U}_h$ and $\hat{V}_h$, and the diagonal matrix $\hat{W}_h$, as

$$\hat{I}_h = \hat{U}_h \hat{W}_h \hat{V}_h^T. \tag{29}$$

The reconstructed image $\hat{I}_h$ should be similar to the N HR training face images. The following squared error $E(i)$ can be used to measure the reconstruction error:

$$E(i) = \sum_{i=1}^{N} \left\| I_h^i - \hat{I}_h \right\|^2, \quad \text{s.t.} \quad \hat{I}_h \downarrow \alpha = I_l. \tag{30}$$

The optimal reconstruction weights β_i, γ_i and ζ_i can be derived by minimizing the following formulation:

$$\begin{aligned}\beta &= \arg\min_{\beta_i,\,\gamma_i,\,\zeta_i} \{E(i)\} \\ &= \arg\min_{\beta_i,\,\gamma_i,\,\zeta_i} \left\{ \sum_{i=1}^{N} \left\| I_h^i - \hat{I}_h \right\|^2 \right\}, \quad \text{s.t.} \quad \hat{I}_h \downarrow \alpha = I_l. \end{aligned} \tag{31}$$

The global constrained least-square problem can be computed using the iterative method in [23], and the determined weights are normalized so that their sum is one.

To further improve the visual quality of the reconstructed HR images, our proposed algorithm also estimates the residual-error matrix $\bar{C}$, which comprises the high-frequency information about a face image, and represents the detailed local features missing from the reconstructed global HR image. This residual information is added as the missing high-frequency information to achieve high-quality face hallucination. Based on our proposed SVD-based mapping model, the matrix $\bar{C}$ can be estimated from the individual residual errors of the selected training samples $\bar{C}^i = I_h^i - \hat{I}_h$, where $\hat{I}_h = \hat{U}_h \hat{W}_h \hat{V}_h^T$, as defined in (19). We use a Gaussian function to measure the similarity of two images, and the weight δ_i reflects the global similarity as

$$\delta_i = \exp\left(\frac{-\left\| I_h^i - \hat{I}_h \right\|^2}{\sigma^2} \right) \tag{32}$$

where $i = 1, \ldots, N$, and σ controls the effect of the gray-level difference between the HR training sample and the reconstructed HR image. The weights δ_i are then normalized so that their sum is equal to 1. After that, the matrix $\bar{C}$ can be computed as

$$\begin{aligned}\bar{C} &= \sum_{i=1}^{N} \delta_i \bar{C}^i \\ &= \sum_{i=1}^{N} \delta_i \left(I_h^i - \hat{I}_h \right). \end{aligned} \tag{33}$$

Having determined the residual-error matrix, the final reconstructed HR face image, denoted by $\bar{I}_h$, can be computed as

$$\bar{I}_h = \hat{I}_h + \bar{C}. \tag{34}$$

With the aid of face verification, this will make the reconstructed HR image more reliable and accurate. In addition, another merit of our proposed algorithm is that face verification can help prevent the production of artifacts and discontinuities during the face-hallucination stage. Based on the reconstructed HR face images and with the potential-field representation of HR face images [39], face verification based on PCA can be conducted. If the query input is the claimed identity, the mapping models learned should be correct and effective for the reconstruction. A high level of verification accuracy can be achieved. Otherwise, i.e., the query is not the claimed identity, the accuracy will be degraded.

B. Simultaneous Face Hallucination and Identification (SHI)

For SHI, Q faces that are the most similar to the input LR face image are first searched from a gallery database of LR–HR pairs based on its singular values [39], as shown in Fig. 1. Suppose that these Q faces belong to M distinct subjects, where $M < Q$, and for each of the M identities, the corresponding mapping models are learned and used to super-resolve the query input. Therefore, M hallucinated HR face images $\bar{I}_h^j$, $j = 1, 2, \ldots, M$, for the LR query are generated using the face hallucination algorithm introduced in Section III-A. Then, the differences between each of the M hallucinated HR face images and the corresponding HR face images of the jth distinct subject, $j = 1, 2, \ldots, M$, in the gallery database are computed using the eigenface method [31].

Fig. 1 shows the proposed framework for the simultaneous hallucination and identification of LR faces. In our framework, the targeted HR U and V matrices of the query input are computed using the mapping models [36] learned from the LR–HR pairs of the respective M distinct subjects. If the query input and the identity of the subject under consideration are the same person, the mapping models should be correct, and hence the HR query face image generated should resemble the corresponding HR face images in the database. Otherwise, the reconstructed HR face is unlikely to be similar to the HR face images of different subjects in the gallery database. By considering face hallucination and identification simultaneously, both the face-hallucination and -identification performances can be improved.

IV. Experimental Results

To verify the effectiveness of the proposed schemes, the combined data set used in [15] and [36] and the LFW database [42], [43] are both used to evaluate the performance of our proposed framework. The facial images in the combined data set were selected from the Georgia Institute of Technology [24], Aleix Martinez and Robert Benavente [25], and face recognition technology [26] databases, which contain 40, 70, and 500 persons, respectively. Five images with a near-frontal view, neutral expression, and different illuminations are randomly chosen from each class for the experiments. Thus, the total number of images in the database is $610 \times 5 = 3050$ images. All the facial images are well aligned based on the position of the two eyes, using the method in [27] and [40]. The parameters λ in (22) and σ in (35) are empirically set at 0.001 and 50, respectively. Our experiments show that using all of the above settings can achieve a satisfactory overall performance. A number of experiments were conducted to verify the effectiveness of our schemes. Our proposed SHV and SHI schemes will be evaluated in Sections IV-A and IV-B, respectively. Furthermore, the experimental results on the LFW database, which are shown in Section IV-C, verify the effectiveness of our SHV and SHI schemes on real-world face images under unconstrained conditions.

A. Experiments on Simultaneous Face Hallucination and Verification (SHV)

The task of face verification is to determine whether a pair of face images belong to the same person. In the experiments,

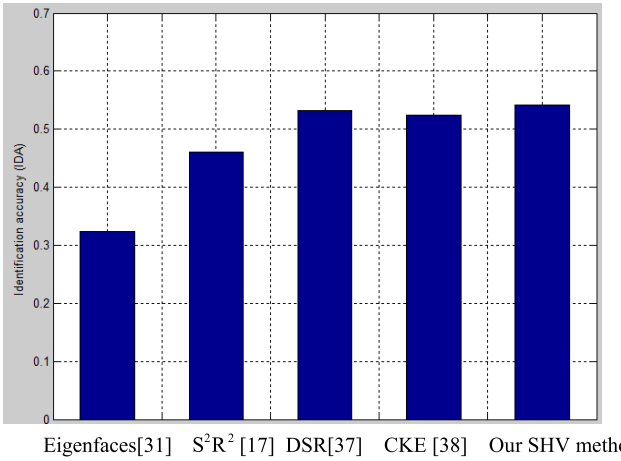

Fig. 2. IDA levels for different algorithms.

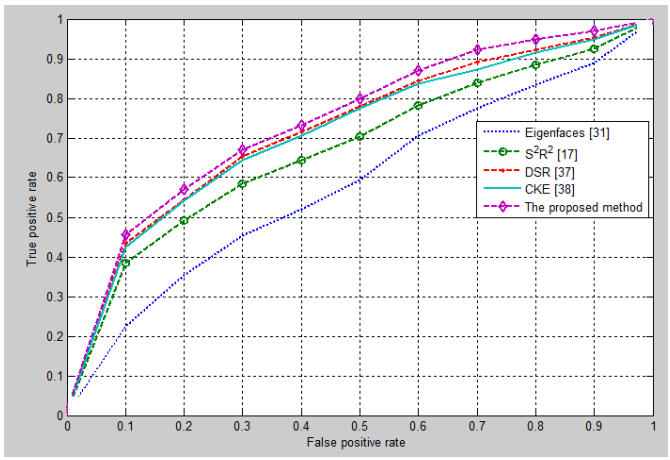

Fig. 3. ROC curve for the different algorithms.

the database consists of 3050 face images of 610 distinct subjects; the original HR facial images are cropped to a size of 72×64 pixels, and the LR faces are of size 18×16 pixels. We followed the standard 10-fold cross-validation over the combined database in the experiments for face verification. The similarity function *SIM* defined in (21) is used to measure the similarity between an input query and the claimed identity in the gallery database for face verification.

In this section, we evaluate the effectiveness of the proposed face-verification approach. The PCA-based algorithm [31] (also known as eigenfaces) is a benchmark for appearance- and image-based face recognition/verification approaches [32]. Therefore, it is used in these experiments to illustrate the effectiveness of our algorithm. As in [33] and [34], the L_1 norm distance metric is used, which is a more suitable distance measure than the Euclidean distance metric (L_2) for PCA-based algorithms. The state-of-the-art algorithm proposed in [17] for the recognition of LR faces, namely, S^2R^2, is employed for comparison. Furthermore, two more state-of-the-art methods—namely, the discriminative constraint-based DSR method [37], which employs the class-label information, and the coupled kernel embedding (CKE) feature-extraction method [38]—are also compared for LR face recognition. For the DSR method [37], images from 610 persons (one per person) are randomly selected to form the training set; the rest of the images form the testing (probe) set. As in [37], the training pairs are clustered using linearity clustering, so that the relationship between the data pairs in each cluster can be linearly approximated. Following [38], 610 images are also randomly selected from the database, and projection directions are trained using the Gaussian-kernel-based CKE algorithm. The kernel parameter is set at 3, and 40 features in the embedding space are extracted for matching.

Fig. 2 shows the identification accuracy (IDA) level, which is the percentage of the probes that are correctly identified by an algorithm. As shown in Fig. 2, the PCA-based algorithm achieves an IDA of only 32.36%. The performance of the S^2R^2 algorithm can further improve the IDA significantly to 46.05%. Both the DSR and CKE methods produce good recognition results compared with that of the PCA-based algorithm: i.e., 53.22% and 52.35%, respectively. Our proposed SHV method can increase the IDA to 54.11%, i.e., achieving a better performance than both the DSR-based algorithm and the CKE algorithm. These experimental results prove that our proposed scheme is effective. The receiver operating characteristic (ROC) curve is shown in Fig. 3. The ROCs show that the proposed SHV method outperforms the other state-of-the-art methods.

The input LR face can be hallucinated using the respective mapping models for the matrices U and V based on the LR–HR face pairs of the claimed identity. For comparison, two interpolation algorithms, namely, the bicubic-interpolation algorithm [29] and the edge-directed interpolation (NEDI) method [30], are applied for face hallucination. Five more state-of-the-art face-hallucination algorithms are also compared with our proposed method: two PCA-based, holistic SR methods (the eigentransformation method [8] and a variant of Park's method [9]); one patch-based method (Freeman's method [3]); Liu's method [10] based on a global parametric model and a local nonparametric model; and an SVD mapping-based method [36]. The version of Park's method used in this paper is different from the original algorithm in [9] in that the training images are warped with reference to the LR input face, rather than with reference to a predefined reference face.

In the experiments, we evaluate all of these methods by reconstructing the HR facial images with a magnification factor of 4. All the testing images of resolution 18×16 pixels are evaluated using the leave-one-out approach. Two objective quality measures, the peak signal-to-noise ratio (PSNR) and structural similarity (SSIM) [28], are used to evaluate the performances of the different methods.

Fig. 4 shows some samples of the reconstruction results generated using the different state-of-the-art face-hallucination algorithms, with a magnification factor $\alpha = 4$. It can be observed from Fig. 4(b) that the bicubic-interpolation algorithm produces the blurriest results. The results in Fig. 4(c) are generated using the NEDI method. However, if a face image has a very LR (i.e., below 18×16 pixels), the NEDI method struggles to distinguish edges, and hence also produces blurry results as compared with the other SR methods.

(a) (b) (c) (d) (e) (f) (g) (h) (i)

Fig. 4. Face-hallucination results reconstructed using different methods with a magnification factor of 4. (a) Original images. (b) Bicubic interpolation. (c) NEDI. (d) Eigentransformation method. (e) Variant of Park's method. (f) Freeman's method. (g) Liu's method. (h) SVD mapping-based method. (i) Our proposed SHV method.

Fig. 4(d) and (e) shows the results generated using the eigentransformation method and the variant of Park's method, respectively, which are both holistic/global face-hallucination methods. Plausible face structures can be clearly inferred in the resulting HR images, which show a better visual quality than both the bicubic-interpolation and the NEDI algorithms. Nevertheless, as the method is purely holistic, it cannot effectively reconstruct the fine individual facial details of those novel testing faces. If a testing face image is very different from the faces in the database, infidelity will occur in the reconstructed HR faces. Park's method employs the morphable face model to capture the shape variations in the novel testing faces, so it outperforms the eigentransformation method. However, the HR textures are still reconstructed in a holistic manner, like in the eigentransformation method. The face-hallucination results using the patch-based SR methods are shown in Fig. 4(f). It can be observed that Freeman's method can provide plausible HR facial images with sharp edges and corners. However, as some of the patches are badly matched and/or conflict with adjacent ones, some structural errors and discontinuities appear in the reconstructed HR images; these errors are typical drawbacks with most patch-based SR methods. Furthermore, patch-based SR usually requires a large number of image-patch pairs for learning, and therefore is computationally expensive. In addition, there are some artifacts in the reconstructed HR images, as shown in Fig. 4(f). Compared with the holistic- and the patch-based approaches, Liu's method [10] utilizes both global and local prior information via a global parametric model and a local nonparametric model. Thus, as shown in Fig. 4(g), the method can produce not only visually plausible face structures, but also fine details and textures like those in the HR training images. However, some parts of the hallucinated faces, such as the mouth, are somewhat different from the original face. This can be partially attributed to the properties of the PCA-based global model used in this approach. Unlike Liu's method, our proposed framework can retain the main energy of the LR faces, and the mapping scheme and the residual matrix can produce HR results with clear details, as shown in Fig. 4(h). In this paper, our proposed framework for the simultaneous verification and hallucination of LR faces can select similar holistic structures and patterns with the LR input during the face-verification stage. It has the advantage of preventing the algorithm from producing artifacts and discontinuities in the reconstruction results, and the estimation of the high-frequency details of the HR face images will become more reliable and effective. As can be observed from Fig. 4(i), plausible HR images with a holistic structure and more details with a better visual quality can be obtained. Table I tabulates the average PSNR and SSIM of the different methods with a magnification factor of 4. The results show that our method is superior, in terms of both measurements, to the other state-of-the-art algorithms.

TABLE I

AVERAGE PSNR AND SSIM OF THE DIFFERENT FACE-HALLUCINATION ALGORITHMS WITH A MAGNIFICATION FACTOR OF 4

Face-hallucination algorithms	PSNR(dB)	SSIM
Bicubic interpolation	19.32	0.5507
NEDI	19.58	0.5585
Eigentransformation method	21.58	0.6392
A variant of Park's method	22.07	0.6410
Freeman's method	22.34	0.6515
Liu's method	21.86	0.6443
Mapping method	22.69	0.6532
Our proposed SHV method.	22.72	0.6627
Our proposed SHI method.	22.83	0.6685

B. Experiments on Simultaneous Face Hallucination and Identification (SHI)

In this section, extensive experiments were performed to evaluate the effectiveness of the proposed SHI algorithm. In the experiments, LR faces of three different resolutions are considered: 18×16, 16×14, and 14×12 pixels, respectively. The number of searched faces Q is set at 40, i.e., $Q = 40$ faces that are the most similar to the input LR face are searched from a gallery database of LR–HR face pairs based on singular values using (11). A face of each subject is randomly selected from the database to form a gallery data set, while the remaining faces are used for testing in the experiments. Eigenfaces are used to measure the differences between each of the M hallucinated HR face images and the corresponding HR face images in the gallery data set.

For comparison, the state-of-the-art methods considered in Section IV-A are also evaluated for LR face recognition. We also evaluate the performances of LR face recognition for super-resolved LR images, first using the SVD-based SR algorithm [36], then using eigenfaces, the local binary pattern (LBP) [44], [45] feature, and the Gabor [46], [47] for face recognition. In other words, face SR and face recognition are performed in two steps, and we denote these three methods as SR + Eigenfaces, SR + LBP, and SR + Gabor, respectively.

TABLE II
AVERAGE RECOGNITION RATES OF 10 DIFFERENT FACE RECOGNITION SCHEMES WITH THE LR FACES OF SIZES 18 × 16 PIXELS AND 16 × 14 PIXELS, RESPECTIVELY

Face sizes / Recognition methods	18×16	16×14	14×12
Eigenfaces[31]	39.44%	37.11%	34. 06%
LBP[45]	42.58%	40.86%	37.33%
Gabor[47]	43.71%	41.75%	38.04%
SR[36]+Eigenfaces[31]	41.25%	39.21%	36.10%
SR[36]+LBP[45]	44.19%	42.63%	41.08%
SR[36]+Gabor[47]	45.20%	43.55%	41.45%
S^2R^2 [17]	55.70%	53.05%	51.88%
DSR[37]	71.66%	70.85%	69.19%
CKE[38]	71.24%	70.32%	68.85%
Our SHI method	72.15%	71.33%	69.50%

Table II tabulates the average recognition rates of the different state-of-the-art algorithms with LR faces at three different resolutions. We have also measured the recognition rates of the PCA-based [31], LBP [45], and Gabor [47] on the LR face images directly. With the use of the SVD-based SR methods first with a magnification factor of 4, the recognition rates of these three methods increase by only 2%–4%. The reason for these performances is that the image resolutions are very low, so the distortions in the super-resolved face images are still significant. Extracting features from these distorted images will further magnify the distortions. For example, the respective improvements are 1.81%, 1.61%, and 1.49% for the three methods with the LR faces of size 18×16 pixels. In contrast, all the four simultaneous hallucination and recognition methods, i.e., S^2R^2 [17], DSR [37], CKE [38], and our SHI method, can achieve much better performances than performing SR and recognition separately. This validates the superior performance of the simultaneous-hallucination and -recognition-based schemes. Our SHI method outperforms the other three methods. When compared with the DSR and CKE methods, our method can achieve an improvement of about 1% in terms of recognition rate.

When the LR faces are reduced to the resolution of 16 × 14 and 14 × 12 pixels, the recognition performances of all the methods degrade. For the resolution of 16 × 14 pixels, the DSR method, and the CKE method achieve recognition rates of 70.85% and 70.32%, respectively; this is much better than that of the PCA-based algorithm, which is 37.11%. The average recognition rate of our proposed SHI method is 71.33%. When the resolution is 14 × 12 pixels, the PCA-based algorithm, the DSR method, and the CKE method achieves recognition rates of 34.06%, 69.19%, and 68.85%, respectively. Our proposed SHI method outperforms all of these methods, and achieves a recognition rate of 69.50%. This shows the effectiveness of our proposed method.

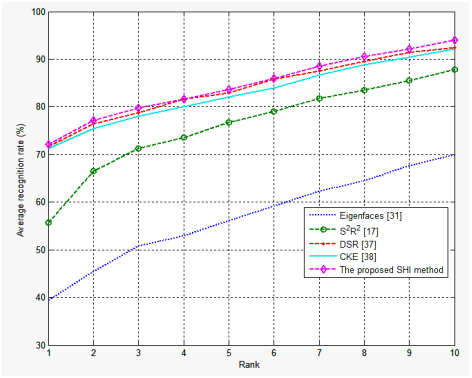

(a)

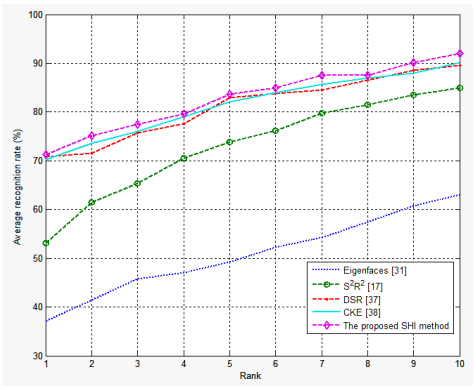

(b)

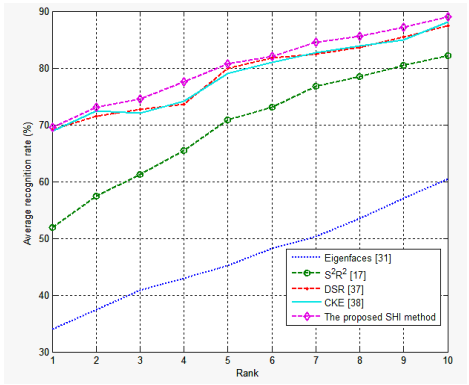

(c)

Fig. 5. CMC curves of the different methods on the combined database with LR faces of sizes. (a) 18 × 16, (b) 16 × 14, and (c) 14 × 12 pixels.

Fig. 5 shows the recognition performance of the different methods in terms of the cumulative matching characteristic (CMC) curve, which evaluates the ranking capability of an identification algorithm, when the resolutions of the LR faces are 18 × 16, 16 × 14, and 14 × 12 pixels, respectively. From these results, we can observe that our proposed SHI method outperforms the other state-of-the-art algorithms.

For simultaneous face hallucination, Table I also tabulates the average PSNR and SSIM of the proposed SHI method with a magnification factor of 4. From Table I, it can be observed that our SHI method is superior to the different state-of-the-art methods in terms of both the average PSNR and SSIM. Table II and Figs. 5–7 show that our proposed SHI method is also superior in terms of the recognition rate and the

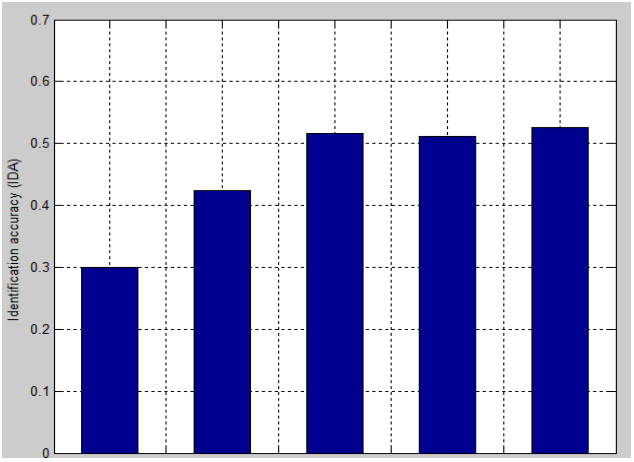

Fig. 6. IDA levels for different algorithms.

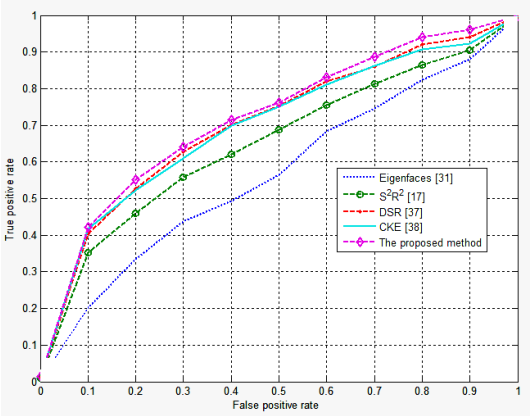

Fig. 7. ROC curves for the different algorithms on the LFW database.

CMC curve compared with other state-of-the-art face-identification algorithms. These experimental results prove that our proposed scheme of SHI is effective, and can achieve an excellent performance.

C. Experimental Results on the Real-World LFW Database

To test the robustness and effectiveness of the proposed schemes on real-world face images under unconstrained conditions, the LFW database [42], [43] (LFW, a database of real-world face images designed to study the problem of unconstrained face recognition) was used to evaluate the performance of our proposed framework. The images in the LFW database were collected in the wild, with variations in pose, lighting condition, resolution, quality, expression, gender, race, occlusion, and make-up [42], [43]. The LFW database contains facial images of 5749 individuals, 1680 of which have more than one image, and 610 of which have more than four images in the database. Four images are randomly chosen from each of the 610 individuals with more than four images in the LFW database for the experiments. All the facial images are well aligned using the deep-funneling method in [43]. Extensive experiments have been conducted on the LFW database to verify the effectiveness of our schemes, and the experimental results of our proposed SHV and SHI schemes are provided in Sections IV-C1 and IV-C2, respectively.

TABLE III
RECOGNITION RATES OF 10 DIFFERENT FACE RECOGNITION METHODS ON THE LFW DATABASE WITH LR FACES OF SIZES 18 × 16, 16 × 14, AND 14 × 12 PIXELS, RESPECTIVELY

Face sizes / Recognition methods	18×16	16×14	14×12
Eigenfaces[31]	36.23%	34.60%	32.09%
LBP[45]	38.44%	36.22%	34.28%
Gabor[47]	39.29%	37.09%	35.34%
SR[36]+Eigenfaces[31]	37.68%	35.70%	33.67%
SR[36]+LBP[45]	40.12%	38.14%	36.26%
SR[36]+Gabor[47]	40.89%	38.65%	36.47%
S^2R^2 [17]	52.95%	51.18%	50.04%
DSR[37]	68.27%	67.42%	65.75%
CKE[38]	68.10%	67.18%	65.13%
Our SHI method	69.20%	68.05%	66.19%

1) Experiments on Simultaneous Face Hallucination and Verification (SHV): For face verification, the 610 individuals LFW database that have more than four images and are well aligned [43] are cropped to a size of 72 × 64 pixels, and the corresponding LR faces are of size 18 × 16 pixels. We have followed the standard 10-fold cross-validation with the LFW database in the experiments for face verification. Our SHV algorithm is compared with the state-of-the-art methods described in Section IV-A, with the same parameters in Section IV-A.

Fig. 6 shows the IDA level on the real-world LFW database. We can see that the PCA-based algorithm achieves an IDA of only 30.03%. The S^2R^2 algorithm can drastically improve the IDA to 42.40%. In contrast to the PCA-based algorithm, both the DSR and CKE methods achieve good recognition results, namely, 51.55% and 51.08%, respectively. It is noted that our proposed SHV method outperforms both the DSR-based algorithm and the CKE algorithm with an IDA of 52.64%. Furthermore, the ROC curves for the different algorithms on the LFW database are shown in Fig. 7. From the results, it can be observed that the proposed SHV method produces a superior performance.

2) Experiments on Simultaneous Face Hallucination and Identification (SHI): To evaluate the proposed SHI algorithm, LR faces of three different resolutions are considered: 18 × 16, 16 × 14, and 14 × 12 pixels, respectively. The state-of-the-art methods used in Section IV-B are also employed for LR face recognition. Table III tabulates the average recognition rates of the different state-of-the-art algorithms on the LFW database for the LR faces at the three different resolutions. We can see that performing SR and

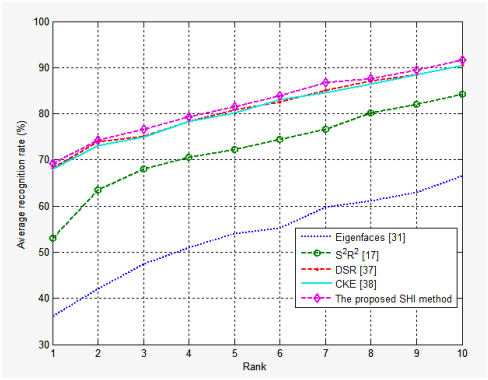

(a)

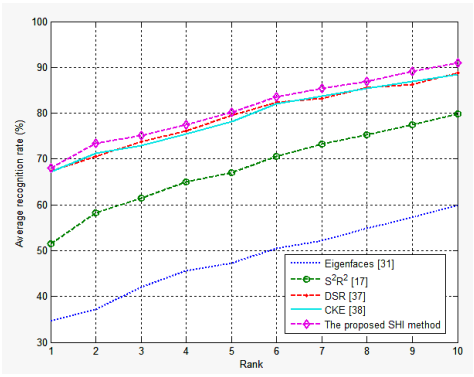

(b)

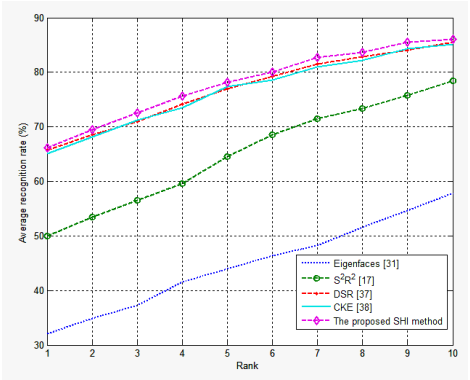

(C)

Fig. 8. CMC curves of the different methods on the LFW database with LR faces of sizes. (a) 18×16, (b) 16×14, and (c) 14×16 pixels.

identification separately, i.e., SR + Eigenfaces, SR + LBP, and SR + Gabor, once again gives a slightly better result than that of LR face recognition without using SR. The four simultaneous hallucination and recognition methods, S^2R^2, DSR, CKE, and our SHI method, produce a much better performance than that of SR identification separately. The experimental results show that the recognition rates of the eigenfaces method are 36.23%, 34.60%, and 32.09% when the LR faces are of resolutions 18×16, 16×14, and 14×12 pixels, respectively. The use of SR methods before face identification can improve the recognition rates by only 1%–2%. The S^2R^2 algorithm achieves much better recognition rates than the eigenfaces method; the corresponding rates are 52.95%, 51.18%, and 50.04%, respectively. Both DSR and CKE can further improve the average recognition rates to 68.27%, 67.42%, and 65.75%, respectively, and 68.10%, 67.18%, and 65.13%, respectively, for the three resolutions. Our proposed SHI method can consistently achieve the best recognition rates of 69.20%, 68.05%, and 66.19%, respectively, which clearly show the effectiveness of our proposed method.

Fig. 8 shows the recognition performances of the different methods in terms of the CMC curves on the LFW database, with the resolutions of the LR faces being 18×16, 16×14, and 14×12 pixels, respectively. The results show that our proposed SHI method is very effective and produces a superior performance when compared with the existing state-of-the-art methods.

V. Conclusion and Discussion

A novel approach for the simultaneous hallucination and recognition of LR faces has been proposed. In our framework, the hallucination and recognition of LR faces are considered simultaneously. Our proposed scheme can retain the holistic structure and the high-frequency details of face images, and it outperforms other, state-of-the-art algorithms in terms of both PSNR and SSIM. The experiments have shown that our proposed method is practicable and can produce plausible HR images with both a holistic structure and high-frequency details. Meanwhile, the experimental results also demonstrate that our proposed simultaneous framework can achieve superior results for both face verification and identification.

References

[1] S. Baker and T. Kanade, "Hallucinating faces," in *Proc. IEEE Int. Conf. Autom. Face Gesture Recognit.*, Mar. 2000, pp. 83–88.
[2] S. Baker and T. Kanade, "Limits on super-resolution and how to break them," *IEEE Trans. Pattern Anal. Mach. Intell.*, vol. 24, no. 9, pp. 1167–1183, Sep. 2002.
[3] W. T. Freeman, T. R. Jones, and E. C. Pasztor, "Example-based super-resolution," *IEEE Comput. Graph. Appl.*, vol. 22, no. 2, pp. 56–65, Mar./Apr. 2000.
[4] G. Dedeoglu, J. August, and T. Kanade, "High-zoom video hallucination by exploiting spatio-temporal regularities," in *Proc. IEEE CVPR*, vol. 2. Jun./Jul. 2004, pp. II-151–II-158.
[5] W. Fan and D.-Y. Yeung, "Image hallucination using neighbor embedding over visual primitive manifolds," in *Proc. IEEE CVPR*, Jun. 2007, pp. 1–7.
[6] K. I. Kim and Y. Kwon, "Example-based learning for single-image super-resolution," in *Proc. 30th DAGM Symp. Pattern Recognit.*, Munich, Germany, 2008, pp. 456–465.
[7] J. Yang, J. Wright, T. S. Huang, and Y. Ma, "Image super-resolution via sparse representation," *IEEE Trans. Image Process.*, vol. 19, no. 11, pp. 2861–2873, Nov. 2010.
[8] X. Wang and X. Tang, "Hallucinating face by eigentransformation," *IEEE Trans. Syst., Man, Cybern. C, Appl. Rev.*, vol. 35, no. 3, pp. 425–434, Aug. 2005.
[9] J.-S. Park and S.-W. Lee, "An example-based face hallucination method for single-frame, low-resolution facial images," *IEEE Trans. Image Process.*, vol. 17, no. 10, pp. 1806–1816, Oct. 2008.
[10] C. Liu, H.-Y. Shum, and W. T. Freeman, "Face hallucination: Theory and practice," *Int. J. Comput. Vis.*, vol. 75, no. 1, pp. 115–134, 2007.
[11] X. Li, K. M. Lam, G. Qiu, L. Shen, and S. Wan, "Example-based image super-resolution with class-specific predictors," *J. Vis. Commun. Image Represent.*, vol. 20, no. 5, pp. 312–322, 2009.
[12] G. Qiu, "A progressively predictive image pyramid for efficient lossless coding," *IEEE Trans. Image Process.*, vol. 8, no. 1, pp. 109–115, Jan. 1999.
[13] G. Qiu, "Interresolution look-up table for improved spatial magnification of image," *J. Vis. Commun. Image Represent.*, vol. 11, no. 4, pp. 360–373, 2000.
[14] X. Ma, J. Zhang, and C. Qi, "Hallucinating face by position-patch," *Pattern Recognit.*, vol. 43, no. 6, pp. 2224–2236, Jun. 2010.

[15] Y. Hu, K.-M. Lam, G. Qiu, and T. Shen, "From local pixel structure to global image super-resolution: A new face hallucination framework," *IEEE Trans. Image Process.*, vol. 20, no. 2, pp. 433–445, Feb. 2011.
[16] A. Akyol and M. Gokmen, "Super-resolution reconstruction of faces by enhanced global models of shape and texture," *Pattern Recognit.*, vol. 45, no. 12, pp. 4103–4116, 2012.
[17] P. H. Hennings-Yeomans, S. Baker, and B. V. K. V. Kumar, "Simultaneous super-resolution and feature extraction for recognition of low-resolution faces," in *Proc. IEEE Conf. Comput. Vis. Pattern Recognit.*, Jun. 2008, pp. 1–8.
[18] R. Epstein, P. W. Hallinan, and A. L. Yuille, "5±2 eigenimages suffice: An empirical investigation of low-dimensional lighting models," in *Proc. Workshop Phys.-Based Modeling Comput. Vis.*, Jun. 1995, pp. 108–116.
[19] Z. Zhang, "Modeling geometric structure and illumination variation of a scene from real images," in *Proc. IEEE ICCV*, Jan. 1998, pp. 1041–1046.
[20] J. Dong and M. Chantler, "Capture and synthesis of 3D surface texture," *Int. J. Comput. Vis.*, vol. 62, nos. 1–2, pp. 177–194, 2005.
[21] M. Jian and J. Dong, "Capture and fusion of 3d surface texture," *Multimedia Tools Appl.*, vol. 53, no. 1, pp. 237–251, 2011.
[22] O. Bretsche, *Linear Algebra With Applications*, 3rd ed. Englewood Cliffs, NJ, USA: Prentice-Hall, Jun. 2004.
[23] P. Wesseling, *An Introduction to Multigrid Methods*. Hoboken, NJ, USA: Wiley, 1992.
[24] Georgia Inst. Technol. *GT Face Database Atlanta*. [Online]. Available: http://www.anefian.com/research/face_reco.htm
[25] A. R. Martinez and R. Benavente, "The AR face database," CVC, Barcelona, Spain, Tech. Rep. 24, 1998. [Online]. Available: http://www2.ece.ohio-state.edu/~aleix/ARdatabase.html
[26] P. J. Phillips, H. Wechsler, J. Huang, and P. J. Rauss, "The FERET database and evaluation procedure for face-recognition algorithms," *Image Vis. Comput.*, vol. 16, no. 5, pp. 295–306, 1998.
[27] K.-W. Wong, K.-M. Lam, and W.-C. Siu, "An efficient algorithm for human face detection and facial feature extraction under different conditions," *Pattern Recognit.*, vol. 34, no. 10, pp. 1993–2004, 2001.
[28] Z. Wang, A. C. Bovik, H. R. Sheikh, and E. P. Simoncelli, "Image quality assessment: From error visibility to structural similarity," *IEEE Trans. Image Process.*, vol. 13, no. 4, pp. 600–612, Apr. 2004.
[29] H. S. Hou and H. Andrews, "Cubic splines for image interpolation and digital filtering," *IEEE Trans. Signal Process.*, vol. 26, no. 6, pp. 508–517, Dec. 1978.
[30] X. Li and M. T. Orchard, "New edge-directed interpolation," *IEEE Trans. Image Process.*, vol. 10, no. 10, pp. 1521–1527, Oct. 2001.
[31] M. Turk and A. Pentland, "Eigenfaces for recognition," *J. Cognit. Neurosci.*, vol. 3, no. 1, pp. 71–86, 1991.
[32] W. Zhao, R. Chellappa, A. Rosenfeld, and P. J. Phillips, "Face recognition: A literature survey," *ACM Comput. Surv.*, vol. 35, no. 4, pp. 399–458, 2003.
[33] H. Moon and P. J. Phillips, "Computational and performance aspects of PCA-based face-recognition algorithms," *Perception*, vol. 30, no. 3, pp. 303–321, 2001.
[34] B. A. Draper, K. Baek, M. S. Bartlett, and J. R. Beveridge, "Recognizing faces with PCA and ICA," *Comput. Vis. Image Understand.*, vol. 91, nos. 1–2, pp. 115–137, 2003.
[35] J. Zou, Q. Ji, and G. Nagy, "A comparative study of local matching approach for face recognition," *IEEE Trans. Image Process.*, vol. 16, no. 10, pp. 2617–2628, Oct. 2007.
[36] M. Jian, K.-M. Lam, and J. Dong, "A novel face-hallucination scheme based on singular value decomposition," *Pattern Recognit.*, vol. 46, no. 11, pp. 3091–3102, 2013.
[37] W. W. W. Zou and P. C. Yuen, "Very low resolution face recognition problem," *IEEE Trans. Image Process.*, vol. 21, no. 1, pp. 327–340, Jan. 2012.
[38] C.-X. Ren, D.-Q. Dai, and H. Yan, "Coupled kernel embedding for low resolution face image recognition," *IEEE Trans. Image Process.*, vol. 21, no. 8, pp. 3770–3783, Aug. 2012.
[39] M. Jian and K.-M. Lam, "Face-image retrieval based on singular values and potential-field representation," *Signal Process.*, vol. 100, pp. 9–15, Jul. 2014.
[40] M. Jian, K.-M. Lam, and J. Dong, "Facial-feature detection and localization based on a hierarchical scheme," *Inf. Sci.*, vol. 262, pp. 1–14, Mar. 2014.
[41] G. B. Huang, M. Ramesh, T. Berg, and E. Learned-Miller, "Labeled faces in the wild: A database for studying face recognition in unconstrained environments," Univ. Massachusetts, Amherst, Amherst, MA, USA, Tech. Rep. 07-49, Oct. 2007.
[42] G. B. Huang, V. Jain, and E. Learned-Miller, "Unsupervised joint alignment of complex images," in *Proc. 11th Int. Conf. Comput. Vis. (ICCV)*, Oct. 2007, pp. 1–8.
[43] G. Huang, M. Mattar, H. Lee, and E. Learned-Miller, "Learning to align from scratch," in *Advances in Neural Information Processing Systems*. Red Hook, NY, USA: Curran & Associates Inc., 2012.
[44] T. Ahonen, A. Hadid, and M. Pietikäinen, "Face description with local binary patterns: Application to face recognition," *IEEE Trans. Pattern Anal. Mach. Intell.*, vol. 28, no. 12, pp. 2037–2041, Dec. 2006.
[45] T. Ahonen, A. Hadid, and M. Pietikäinen, "Face recognition with local binary patterns," in *Proc. Eur. Conf. Comput. Vis.*, 2004, pp. 469–481.
[46] J. P. Jones and L. A. Palmer, "An evaluation of the two-dimensional Gabor filter model of simple receptive fields in cat striate cortex," *J. Neurophysiol.*, vol. 58, no. 6, pp. 1233–1258, 1987.
[47] C. Liu and H. Wechsler, "Gabor feature based classification using the enhanced Fisher linear discriminant model for face recognition," *IEEE Trans. Image Process.*, vol. 11, no. 4, pp. 467–476, Apr. 2002.

Muwei Jian received the Ph.D. degree from the Department of Electronic and Information Engineering, The Hong Kong Polytechnic University, Hong Kong, in 2014.

He joined the Department of Computer Science and Technology, Ocean University of China, Qingdao, China, as a Lecturer, in 2015. His research interests include image and video processing, wavelet analysis, 3-D multimedia analysis, and human face hallucination/recognition.

Dr. Jian has served as a reviewer for several international SCI-indexed journals, such as *Pattern Recognition*, *Computers in Industry*, *The Imaging Science Journal*, *Machine Vision and Applications*, and *Multimedia Tools and Applications*.

Kin-Man Lam (SM'14) received the Associateship in electronic engineering from The Hong Kong Polytechnic University, Hong Kong, in 1986; the M.Sc. degree in communication engineering from the Department of Electrical Engineering, Imperial College of Science, Technology and Medicine, London, U.K., in 1987; and the Ph.D. degree from the Department of Electrical Engineering, University of Sydney, Sydney, NSW, Australia, in 1996.

He was a Lecturer with the Department of Electronics Engineering, The Hong Kong Polytechnic University, from 1990 to 1993. He joined the Department of Electronics and Information Engineering, The Hong Kong Polytechnic University, as an Assistant Professor, in 1996, where he became an Associate Professor in 1999. He was involved in professional activities. He is currently a Professor with The Hong Kong Polytechnic University. His research interests include human face recognition, image and video processing, and computer vision.

Prof. Lam has been a member of the Organizing Committee or Program Committee of many international conferences. He was a Secretary of the IEEE International Conference on Acoustics, Speech, and Signal Processing in 2003, the Technical Chair of the International Symposium on Intelligent Multimedia, Video and Speech Processing in 2004, the Technical Co-Chair of the International Symposium on Intelligent Signal Processing and Communication Systems in 2005, a Secretary of the International Conference on Image Processing in 2010, the Technical Co-Chair of the Pacific-Rim Conference on Multimedia in 2010, and the General Co-Chair of the IEEE International Conference on Signal Processing, Communications and Computing in Hong Kong in 2012. He was the Chairman of the IEEE Hong Kong Chapter of Signal Processing from 2006 to 2008. He has served as an Associate Editor of IEEE TRANSACTIONS ON IMAGE PROCESSING and the Director of Student Services of the IEEE Signal Processing Society. He is the Vice President of Member Relations and Development of the Asia-Pacific Signal and Information Processing Association (APSIPA) and the Director of Membership Services of the IEEE Signal Processing Society. He is an Area Editor of *IEEE Signal Processing Magazine* and an Associate Editor of *Digital Signal Processing*, *APSIPA Transactions on Signal and Information Processing*, and *EURASIP International Journal on Image and Video Processing*. He is also an Editor of *HKIE Transactions*.